

Scattered waves fuel emergent activity

Ella M. King*,^{1,2} Mia C. Morrell*,¹ Jacqueline B. Sustiel,¹ Matthew Gronert,¹ Hayden Pastor,¹ and David G. Grier¹

¹*Department of Physics and Center for Soft Matter Research,
New York University, New York, NY 10003, USA*

²*Simons Junior Fellow, 160 5th Ave, New York, NY 10010, USA*
(Dated: May 9, 2024)

Particles that scatter waves interact through the waves they scatter. We establish that wave-mediated interactions between dissimilar particles are *generically* nonreciprocal. This apparent violation of Newton’s third law is allowed because the pair of particles does not constitute a closed system; the balance of the system’s momentum is carried away by the scattered wave. Nonreciprocal interactions enable collections of scatterers to transduce energy out of a wave and use it to power their own motion. Such wave-matter composites therefore are a form of active matter. Their activity, however, is not an inherent property of the individual particles, nor are the particles simply driven by the wave. Instead, the particles’ collective motion is an emergent property of their state of organization. This kind of emergent activity should appear in any context where objects scatter waves. As a concrete example, we combine analysis, experiment and simulation to demonstrate how nonreciprocity and emergent activity arise in collections of acoustically levitated spheres.

I. INTRODUCTION

Waves, whether sound waves, light waves, or even gravitational waves, exert forces and torques on the objects that scatter them. Pairs of objects immersed in a wave experience an interaction mediated by the exchange of scattered waves. Here we demonstrate that such wave-mediated pair interactions are generically nonreciprocal and therefore are not constrained by Newton’s third law [1]. This violation is permitted because the objects do not constitute a closed system: scattered waves carry away the balance of their momentum into degrees of freedom that go unrecorded. The objects’ visible degrees of freedom consequently can behave counterintuitively.

The nonreciprocity of wave-mediated interactions has profound implications for self-organization in any context where externally excited waves contribute to a system’s dynamics. Unbalanced forces enable pairs of particles to harvest energy from the incident wave and use it to drive their motion. The ability to transduce energy from the environment is the defining characteristic of active matter [2–4]. This form of wave-mediated activity, however, is inherent neither to the particles nor to the wave. Instead, wave-mediated activity is an emergent property of the system’s state of organization that appears not to have been previously reported. We formulate and experimentally demonstrate emergent activity using acoustically levitated spheres as a model system. Our findings may explain some of the anomalous behavior reported in previous studies such as self-propulsion of acoustically levitated clusters [5] and spontaneous rotation of acoustically levitated rafts [6]. More generally, nonreciprocity and emergent activity can arise in any context where waves interact with matter.

Many active systems exhibit nonreciprocal interactions, and therefore have interesting and counterintuitive collective properties. Nonreciprocity arising from activity has been used to control heat flux in nanoparticles [7], to induce odd elasticity and odd viscosity in active solids

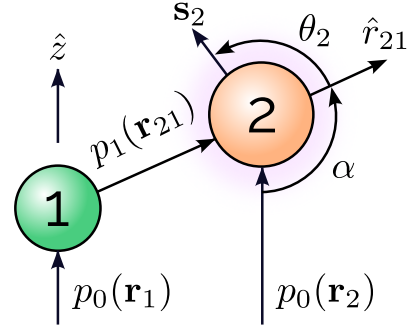


FIG. 1. Geometry for computing the wave-mediated forces. Particle 1 scatters a portion of the incident sound wave to its neighbor at \mathbf{r}_2 . The scattered wave interferes with the incident wave and therefore influences the force experienced by particle 2. Formulating this influence is facilitated by defining a spherical coordinate system centered on particle 2 and aligned with the separation between the particles, $\mathbf{r}_{21} = \mathbf{r}_2 - \mathbf{r}_1$.

and fluids [8], and to generate traveling waves in active mixtures [9]. In all of these cases, activity is an intrinsic property and nonreciprocity is emergent. Systems governed by wave-mediated interactions, by contrast, inherently have nonreciprocal dynamics, so that activity is an emergent property. Emergent activity consequently can be readily tune and controlled by experimentally accessible parameters, including the properties of the incident wave and the sizes, shapes and compositions of the immersed particles.

II. WAVE-MEDIATED FORCES

Our system consists of discrete particles immersed in a harmonic sound wave at frequency ω whose spatial structure is described by the pressure field, $p_0(\mathbf{r})$. An analogous formulation can be provided for objects scattering

light, water ripples, or any other harmonic wave. The total acoustic pressure field, $p(\mathbf{r})$, is the superposition of $p_0(\mathbf{r})$ and the waves scattered by the particles. The pressure serves as the scalar potential for the sound's velocity in the approximation that the fluid's viscosity may be neglected [10–13],

$$\mathbf{v}(\mathbf{r}) = -\frac{i}{\rho_0\omega}\nabla p, \quad (1a)$$

where ρ_0 is the density of the fluid medium.

Both the pressure and the velocity contribute to the time-averaged stress tensor in the fluid medium [13, 14],

$$\underline{\sigma}(\mathbf{r}) = \frac{1}{2} \left[\kappa_0 |p(\mathbf{r})|^2 - \rho_0 |\mathbf{v}(\mathbf{r})|^2 \right] \underline{I} + \rho_0 \mathbf{v}^* \otimes \mathbf{v}, \quad (1b)$$

where \underline{I} is the identity tensor and where $\kappa_0 = (\rho_0 c_0^2)^{-1}$ is the isentropic compressibility of the medium given its speed of sound, c_0 . The first term on the right-hand side of Eq. (1b) accounts for the Lagrangian energy density of the sound. The second is the Reynolds stress [10, 15]. Integrating the normal component of the stress over the surface, S_j , of the j -th particle yields the time-averaged force experienced by that particle:

$$\mathbf{F}_j = -\frac{1}{2} \Re \left\{ \oint_{S_j} \underline{\sigma}(\mathbf{r}) \cdot \hat{\mathbf{n}} d^3r \right\}, \quad (1c)$$

where $\hat{\mathbf{n}}(\mathbf{r})$ is the unit normal to the particle's surface. In practice, \mathbf{F}_j is most conveniently obtained by setting $p(\mathbf{r}) = \Pi_j(\mathbf{r})$ in Eq. (1), where $\Pi_j(\mathbf{r})$ is the pressure inside the j -th particle. We obtain an expression for this interior field by matching boundary conditions in a multiple expansion.

Referring to Fig. 1, the pressure wave incident on particle j can be expressed as

$$p_0(\mathbf{s}_j) = p_0 \sum_{\ell=0}^{\infty} \sum_{m=-\ell}^{\ell} a_{\ell}^m(k\mathbf{r}_j) j_{\ell}(ks_j) Y_{\ell}^m(\theta_j, \phi), \quad (2)$$

in a spherical coordinate system, $\mathbf{s}_j = (s_j, \theta_j, \phi) = \mathbf{r} - \mathbf{r}_j$, centered on the particle's location, \mathbf{r}_j and oriented along the pressure wave's wave vector, $\hat{\mathbf{k}}$, at the particle's position. Distances in Eq. (2) are scaled by the wave number in the medium, $k = \omega/c_0$. The wave's geometry is expressed in terms of spherical Bessel functions of the first kind, $j_{\ell}(kr)$, and spherical harmonics, $Y_{\ell}^m(\theta, \phi)$. Its structure is encoded in the beam shape coefficients, $a_{\ell}^m(k\mathbf{r}_j)$, in the particle's frame of reference.

The wave scattered by particle j similarly can be expressed as a multipole expansion [16],

$$p_j(\mathbf{s}_j) = p_0 \sum_{\ell=0}^{\infty} \sum_{m=-\ell}^{\ell} a_{\ell}^m(k\mathbf{r}_j) B_{\ell m}^{(j)} h_{\ell}(ks_j) Y_{\ell}^m(\theta_j, \phi), \quad (3)$$

in terms of spherical Hankel functions of the first kind, $h_{\ell}(kr)$. The scattering coefficients, $B_{\ell m}^{(j)}$, are obtained

by requiring the pressure and the normal component of the velocity to be continuous at the particle's surface. These boundary conditions also yield the transmission coefficients, $D_{\ell m}^{(j)}$, that establish the interior pressure,

$$\Pi_j(\mathbf{s}_j) = p_0 \sum_{\ell=0}^{\infty} \sum_{m=-\ell}^{\ell} a_{\ell}^m(k\mathbf{r}_j) D_{\ell m}^{(j)} j_{\ell}(k_j s_j) Y_{\ell}^m(\theta_j, \phi). \quad (4)$$

Distances within the particle are scaled by $k_j = \omega/c_j$, where c_j is the interior speed of sound.

A. Scattering by spheres

For simplicity and clarity, we consider the special case in which the particles are homogeneous spheres of radius a_j , density ρ_j and interior speed of sound c_j . Continuity of the pressure at the j -th sphere's surface requires

$$p_0(\mathbf{s}_j) + p_j(\mathbf{s}_j)|_{s_j=a_j} = \Pi_j(\mathbf{s}_j)|_{s_j=a_j}. \quad (5a)$$

Continuity of the normal component of the velocity requires

$$\rho_0 \frac{\partial}{\partial s_j} [p_0(\mathbf{s}_j) + p_j(\mathbf{s}_j)] \Big|_{s_j=a_j} = \rho_j \frac{\partial}{\partial s_j} \Pi_j(\mathbf{s}_j) \Big|_{s_j=a_j}. \quad (5b)$$

In agreement with previous studies [17], we find these boundary conditions are satisfied by the scattering and transmission coefficients,

$$B_{\ell m}^{(j)} = \frac{j_{\ell}(ka_j) j'_{\ell}(k_j a_j) - \lambda_j j'_{\ell}(ka_j) j_{\ell}(k_j a_j)}{\lambda_j h'_{\ell}(ka_j) j_{\ell}(k_j a_j) - h_{\ell}(ka_j) j'_{\ell}(k_j a_j)}, \quad (6)$$

$$D_{\ell m}^{(j)} = \frac{\rho_0 j_{\ell}(ka_j) h'_{\ell}(ka_j) - j'_{\ell}(ka_j) h_{\ell}(ka_j)}{\rho_j h'_{\ell}(ka_j) j_{\ell}(k_j a_j) - \lambda_j h_{\ell}(ka_j) j'_{\ell}(k_j a_j)}, \quad (7)$$

respectively, where primes denote derivatives with respect to arguments and where $\lambda_j = \rho_j c_j / (\rho_0 c_0)$ is the specific acoustic impedance of the particle relative to that of the medium.

B. The force on a sphere

Substituting Eq. (7) into Eq. (4) yields the pressure within the j -th sphere. The force on that sphere then follows from Eq. (1),

$$\mathbf{F}_j = F_0 (ka_j)^3 \sum_{\ell=0}^{\infty} \sum_{m=-\ell}^{\ell} J_{\ell m}^{(j)} d_{\ell m}^{(j)} d_{\ell+1, m}^{(j)*} \hat{\mathbf{k}}, \quad (8)$$

where $d_{\ell m}^{(j)} = a_{\ell}^m(k\mathbf{r}_j) D_{\ell m}^{(j)}$ are the beam shape coefficients for the interior wave. The magnitude of the force is set by a prefactor,

$$F_0 = \frac{p_0^2}{\rho_0 \omega^2}, \quad (9)$$

that depends on properties of the sound wave in the medium. Coupling between multipole moments medi-

ated by scattering at the sphere's surface is described by the coefficients,

$$J_{\ell m}^{(j)} = -\frac{\rho_j}{2} \sqrt{\frac{(\ell+m+1)(\ell-m+1)}{(2\ell+3)(2\ell+1)}} \left\{ \left[\frac{\kappa_0}{\kappa_j} x_j^2 + m \frac{\rho_j}{\rho_0} \frac{(\ell+m)!}{(\ell-m)!} \frac{\ell+1}{\ell-m+1} \right] j_\ell(x_j) j_{\ell+1}(x_j) \right. \\ \left. + (\ell+2) x_j j'_\ell(x_j) j_{\ell+1}(x_j) - \ell x_j j_\ell(x_j) j'_{\ell+1}(x_j) + \frac{\rho_0}{\rho_j} x_j^2 j'_\ell(x_j) j'_{\ell+1}(x_j) \right\}, \quad (10)$$

where $x_j = k_j a_j$. Equation (10) differs from previously reported expressions for the coupling coefficients [10, 14, 16], which were derived under the assumption of azimuthal symmetry and only include terms with $m = 0$. The additional terms in the complete expression for $J_{\ell m}^{(j)}$ are required for more general pressure waves, including the scattered waves exchanged by pairs of particles. This expression is analogous to Eq. (2.32) in Ref. [17], but projects the force along \hat{k} , which is useful for computing interactions.

C. A sphere in a standing wave

As an illustrative example, we use this formalism to evaluate the force exerted on the j -th sphere by a plane standing wave,

$$p_0(\mathbf{r}) = p_0 \sin(kz), \quad (11)$$

whose axis is aligned in the vertical direction, \hat{z} . The incident field's beam shape coefficients [13, 16],

$$a_\ell^m(k\mathbf{r}_j) = 4\pi(-1)^{\ell-m} \sin\left(kz_j - \ell\frac{\pi}{2}\right) Y_\ell^{-m}(0,0), \quad (12)$$

depend on the particle's height, z_j , above the nodal plane at $z = 0$. In the absence of other particles, we can use Eq (8) to compute the force on particle j due to the incident field:

$$\mathbf{F}_{j0} = \frac{\pi}{3} F_0 (ka_j)^3 \left(\frac{\kappa_j}{\kappa_0} - \frac{3\rho_j}{\rho_0 + 2\rho_j} \right) \sin(2kz_j) \hat{z}. \quad (13)$$

Equation (13) includes only terms at monopole order ($\ell = 0$) in the multipole expansion, and agrees with the expression reported in Ref. [17]. Contributions from multipole orders $\ell \geq 1$ scale as $(ka_j)^5$ and therefore can be neglected for spheres that are smaller than the wavelength of sound, $ka_j < 1$.

The force described by Eq. (13) differentiates bubbles ($\rho_j < \rho_0$ and $\kappa_j > \kappa_0$) from dense spheres ($\rho_j > \rho_0$ and $\kappa_j < \kappa_0$). The prefactor of \mathbf{F}_{j0} is positive for bubbles, which therefore are stably trapped at antinodes of the pressure field. Dense spheres, by contrast, have a

negative prefactor and are stably trapped at nodes. This distinction qualitatively differentiates the wave-mediated interaction experienced by bubbles in a standing wave from that experienced by dense spheres.

III. WAVE-MEDIATED INTERACTIONS

A. Acoustic forces on a pair of particles

As illustrated schematically in Fig. 1, the wave scattered by particle 1 interferes with the external wave incident on particle 2,

$$p(\mathbf{r}) = p_0(\mathbf{r}) + p_1(\mathbf{r} - \mathbf{r}_1), \quad (14)$$

and therefore contributes to the force on that particle. In principle, the second particle scatters a portion of $p(\mathbf{r})$ back to the first, giving rise to a hierarchy of exchanged waves. For simplicity, we invoke the first Born approximation and consider only the first exchange of scattered waves.

Computing the force on particle 2 requires an expression for the interior pressure, $\Pi_2(\mathbf{r})$, and thus an expression for the first particle's scattered wave, $p_1(\mathbf{r} - \mathbf{r}_1)$, in spherical coordinates, \mathbf{s}_2 centered on \mathbf{r}_2 . To facilitate the projection, we align the axis of the coordinate system along $\mathbf{r}_{21} = \mathbf{r}_2 - \mathbf{r}_1$, as shown in Fig. 1. In this coordinate system, the pressure wave scattered by particle 1,

$$p_1(\mathbf{s}_2) = p_0 \sum_{n=0}^{\infty} \sum_{m=-n}^n \sum_{\ell=|m|}^{\infty} a_n^m(k\mathbf{r}_1) B_{nm}^{(1)} K_{n\ell m}(kr_{21}) \\ \times j_\ell(ks_2) Y_\ell^m(\theta_2, \phi), \quad (15a)$$

depends on the scattering coefficients, B_{1n}^m , for particle 1 and includes projection coefficients [18],

$$K_{\ell nm}(kr) = \sum_{s=0}^{n+\ell} \sqrt{\frac{2s+1}{4\pi}} C(\ell m | s 0 | n m) h_s(kr), \quad (15b)$$

that account for the particles' separation, kr . The projection coefficients are expressed in terms of Wigner 3- j

symbols through

$$C(\ell m|s_0|nm) = i^{-\ell+s+n}(-1)^m \times \sqrt{4\pi(2n+1)(2s+1)(2\ell+1)} \times \begin{pmatrix} \ell & s & n \\ 0 & 0 & 0 \end{pmatrix} \begin{pmatrix} \ell & s & n \\ -m & 0 & m \end{pmatrix}. \quad (15c)$$

The upper limit of the sum in Eq. (15b) reflects selection rules for the Wigner 3-j symbols [19].

The pressure inside particle 2,

$$\Pi_2(\mathbf{s}_2) = p_0 \sum_{\ell=0}^{\infty} \sum_{m=-\ell}^{\ell} b_{\ell m}^{(21)} D_{\ell m}^{(2)} j_{\ell}(k_2 s_2) Y_{\ell}^m(\theta_2, \phi), \quad (16)$$

depends on that particle's transmission coefficients, $D_{\ell m}^{(2)}$, as well as the beam-shape coefficients of the incident wave,

$$b_{\ell m}^{(21)} = a_{\ell}^m(k\mathbf{r}_2) + \sum_{n=0}^{\infty} K_{n\ell m}(kr_{21}) a_n^m(k\mathbf{r}_1) B_{nm}^{(1)}, \quad (17)$$

which is superposition of the external wave and the wave scattered by particle 1. The total force on particle 2, \mathbf{F}_2 , follows from Eq. (1) using the multipole coefficients $d_{\ell m}^{(21)} = b_{\ell m}^{(21)} D_{\ell m}^{(2)}$. The projection of that force along \hat{r}_{21} ,

$$\mathbf{F}_2 \cdot \hat{r}_{21} = \sum_{\ell=0}^{\infty} \sum_{m=-\ell}^{\ell} J_{\ell m}^{(2)} d_{\ell m}^{(21)} d_{\ell+1, m}^{(21)*}, \quad (18)$$

includes contributions arising from the incident wave alone, the scattered wave alone, and interference between those two waves.

The force on particle 1, projected into the same direction, follows by exchange of indexes,

$$\mathbf{F}_1 \cdot \hat{r}_{21} = - \sum_{\ell=0}^{\infty} \sum_{m=-\ell}^{\ell} J_{\ell m}^{(1)} d_{\ell m}^{(12)} d_{\ell+1, m}^{(12)*}. \quad (19)$$

Any imbalance between \mathbf{F}_1 and \mathbf{F}_2 gives rise to a net force on the particles' center of mass,

$$\Delta \mathbf{F}_{21}(\mathbf{r}_{21}) \cdot \hat{r}_{21} = (\mathbf{F}_1 + \mathbf{F}_2) \cdot \hat{r}_{21}. \quad (20)$$

The appearance of such an imbalance does not necessarily provide insight into the nature of wave-mediated pair interactions because it could reflect an unequal influence of the incident wave on the two particles, depending on their positions within the pressure field.

To cast a spotlight on the pair interaction, we focus on the much-studied [10, 14, 20–23] special case of two spheres levitated in a standing plane wave. For simplicity, we neglect gravity and assume that the spheres are localized at the same plane within the standing wave. Referring again to Fig. 1, this choice corresponds to $\alpha = \pi/2$. Orienting the beam this way slightly modifies the beam shape coefficients in Eq 12, where the argument

to the spherical harmonic becomes $Y_{\ell}^m(\frac{\pi}{2}, 0)$. Any force due to the incident wave therefore will be orthogonal to the projection of the spheres' wave-mediated interaction, $\mathbf{F}_{21}(\mathbf{r}_{21})$ along \hat{r}_{21} . The pair interaction in this geometry historically has been dubbed the secondary Bjerknes interaction for bubbles [21] and the König force for dense spheres [20]. We will formulate this force in the Rayleigh approximation, $ka_1, ka_2 < 1$, so that we may reasonably truncate the multipole expansion at quadrupole order, $\ell = 2$.

B. Two bubbles in a standing plane wave

Bubbles are less dense than the medium ($\rho_j < \rho_0$) and more compressible ($\kappa_j > \kappa_0$) and so are localized at antinodes of the pressure wave. To leading nontrivial order in the small parameters, ka_j , ρ_j/ρ_0 and κ_0/κ_j , Eq. (18) predicts that the wave-mediated interaction between two coplanar bubbles separated by distance r in an antinodal plane of a standing plane wave is

$$\mathbf{F}_{21}^B(r) = -\frac{2\pi}{9} F_0 f_0^{(1)} f_0^{(2)} (ka_1)^3 (ka_2)^3 \Phi_B(kr) \hat{r} \quad (21a)$$

where $f_0^{(j)} = 1 - \kappa_j/\kappa_0$ is the monopole scattering coefficient [24] for bubble j . This expression specifically describes the force on bubble 2 that can be ascribed to its interaction with bubble 1. The dependence on the bubbles' separation,

$$\Phi_B(kr) = \frac{\cos(kr) + kr \sin(kr)}{(kr)^2}, \quad (21b)$$

shows that the wave-mediated interaction is attractive when the bubbles are near contact and changes sign at larger separations. Equation (21) includes terms up to dipole order ($\ell = 1$) in the multipole expansion and agrees with previously reported expressions [14, 17] for this interaction at the same level of approximation. Reference [10] proposes a different numerical prefactor because its derivation imposes axisymmetry on the pressure field, which is not appropriate for multipole contributions with $m \neq 0$. Equation (21) reduces to the standard expression for the secondary Bjerknes force [16, 21, 23] at small separations. Most notably, the secondary Bjerknes interaction is reciprocal, $\mathbf{F}_{21}^B(r) = -\mathbf{F}_{12}^B(r)$, even for bubbles of different sizes and compositions.

Previous studies of inhomogeneous pair interactions went no further than the level of approximation embodied in Eq. (21) and therefore concluded that the interaction is reciprocal [16, 17]. References [23] and [5] note the existence of nonreciprocal acoustic interaction forces, but suggests they are too small to be significant, and attribute observable nonreciprocal effects to complex multiple scattering mechanisms. In fact, the nature of the pair interaction changes qualitatively when higher-order multipole contributions are taken into account. These changes are present even in the first scattering event, and

take a surprisingly elegant form. The quadrupole-order expression from Eq. (18),

$$\mathbf{F}_{21}(r) = \mathbf{F}_{21}^B(r) (1 + \chi_{21}^B) \quad (22)$$

introduces a correction,

$$\chi_{21}^B = \alpha_{21}^B + \beta_{21}^B (ka_1)^2 + \gamma_{21}^B (ka_2)^2 \quad (23a)$$

that depends on the bubbles' compositions and sizes. Additional terms and higher multipole contributions all appear at $\mathcal{O}\{(ka_j)^3\}$ and can be neglected. Expressing the coefficients to leading nontrivial order yields

$$\alpha_{21}^B = -\frac{3}{2} \frac{\kappa_0 \rho_2^2}{\kappa_2 \rho_0^2} \quad (23b)$$

$$\beta_{21}^B = -\frac{2}{3} + \frac{1}{3} \frac{\kappa_1}{\kappa_0} + \frac{1}{15} \frac{\rho_1}{\rho_0} \left(1 + \frac{\kappa_1}{\kappa_0}\right) + \frac{1}{10} \frac{\kappa_0}{\kappa_1} \quad (23c)$$

$$\gamma_{21}^B = -\frac{2}{3} + \frac{1}{3} \frac{\kappa_2}{\kappa_0} + \frac{1}{15} \frac{\rho_2}{\rho_0} \left(1 + \frac{\kappa_2}{\kappa_0}\right) + \frac{1}{20} \frac{\kappa_0}{\kappa_2}, \quad (23d)$$

from which we conclude that $\chi_{21}^B \neq \chi_{12}^B$. This establishes that the wave-mediated interaction between pairs of bubbles is nonreciprocal if the bubbles have different sizes or compositions. Importantly, these nonreciprocal forces are not necessarily small compared to the reciprocal part of the secondary Bjerknes force.

The discovery reported in Eq. (23) complements a recent report of nonreciprocal wave-mediated interactions that arise from the viscosity of the medium [25]. Equation (23) reveals that nonreciprocity is not predicated on dissipative processes in viscous flows, but instead emerges naturally as a consequence of interference between the incident and scattered waves. The same general mechanism that applies to bubbles in dense media therefore should apply as well to dense particles levitated in light inviscid media, such as air.

C. Two dense spheres in a standing plane wave

Spheres that are denser than the fluid medium will be localized in one of the nodal planes of the standing wave. The leading-order expression for the wave-mediated force on particle 2 due to particle 1,

$$\mathbf{F}_{21}^K(r) = -\frac{2\pi}{3} F_0 f_1^{(1)} f_1^{(2)} (ka_1)^3 (ka_2)^3 \Phi_K(kr) \hat{r}, \quad (24a)$$

is known as the König interaction [20] and broadly resembles the secondary Bjerknes interaction between bubbles from Eq. (21). The König interaction is shorter-ranged,

$$\Phi_K(kr) = \frac{[1 - \frac{1}{3}(kr)^2] \cos(kr) + kr \sin(kr)}{(kr)^4}, \quad (24b)$$

and its scale is set by the particles' dipole coupling coefficients [24], $f_1^{(j)} = (\rho_0 - \rho_j)/(\rho_0 + 2\rho_j)$. These differences arise because bubbles principally scatter the pressure field, with a leading contribution from monopole

scattering, while dense particles principally scatter the dipolar velocity field. This expression agrees with previously published results for the special case of identical particles [23]. The asymmetric case appears not to have been reported previously. As for bubbles, the spheres' interaction is reciprocal to leading order and is attractive at small separations.

Equation (24) is appropriate for particles that are substantially more dense and less compressible than the medium, $\rho_0/\rho_j < 1$, $\kappa_j/\kappa_0 < 1$. As for the secondary Bjerknes interactions between bubbles, the leading-order correction for dense spheres,

$$\mathbf{F}_{21}(r) = \mathbf{F}_{21}^K(r) (1 + \chi_{21}^K), \quad (25)$$

breaks the reciprocity of the standard König expression with a term,

$$\chi_{21}^K = \alpha_{21}^K + \beta_{21}^K (ka_1)^2 + \gamma_{21}^K (ka_2)^2, \quad (26a)$$

that identifies roles for the spheres' sizes and compositions through the leading order nontrivial coefficients,

$$\alpha_{21}^K = -1 + \frac{\rho_0}{\rho_2} \quad (26b)$$

$$\beta_{21}^K = -\frac{3}{10} \frac{\rho_0}{\rho_2} \left(1 + \frac{3}{2} \frac{\rho_0}{\rho_1}\right) \quad (26c)$$

$$\gamma_{21}^K = 1 + \frac{7}{90} \frac{\rho_0}{\rho_2}. \quad (26d)$$

Equation (26) complements Eq. (23) by establishing that the wave-mediated interaction between dense spheres also is nonreciprocal if the spheres differ in composition or size. As in the bubble case, nonreciprocal interactions between dense spheres are not necessarily weak. In particular, these forces can be strong if the reduced radii of the dense particles are close to 1, or if their density is close to that of the medium.

IV. EMERGENT ACTIVITY

A. The principle of emergent activity

Nonreciprocal forces are nonconservative. The net force acting on the particles' center of mass,

$$\Delta \mathbf{F}_{21}(\mathbf{r}_{21}) = (\chi_{21} - \chi_{12}) \mathbf{F}_{21}^R(\mathbf{r}_{21}) \quad (27)$$

accelerates the pair along the line connecting their centers. Here, $\mathbf{F}_{21}^R(\mathbf{r}_{21})$ is the reciprocal part of the force on particle 2 due to particle 1 and χ_{21} captures the nonreciprocity of the wave-mediated pair interaction. The nonreciprocal part of the pair interaction tends to be weaker than the reciprocal part, which means that pairs tend to be drawn into contact by the reciprocal part of their interaction and then are accelerated as a unit by the nonreciprocal part. For bubbles composed of the same material, the center-of-mass force reduces to

$$\Delta \mathbf{F}_{21}(\mathbf{r}_{21}) = \frac{1}{20} \frac{\kappa_0}{\kappa_j} [(ka_1)^2 - (ka_2)^2] \Delta \mathbf{F}_{21}^B(\mathbf{r}_{21}), \quad (28)$$

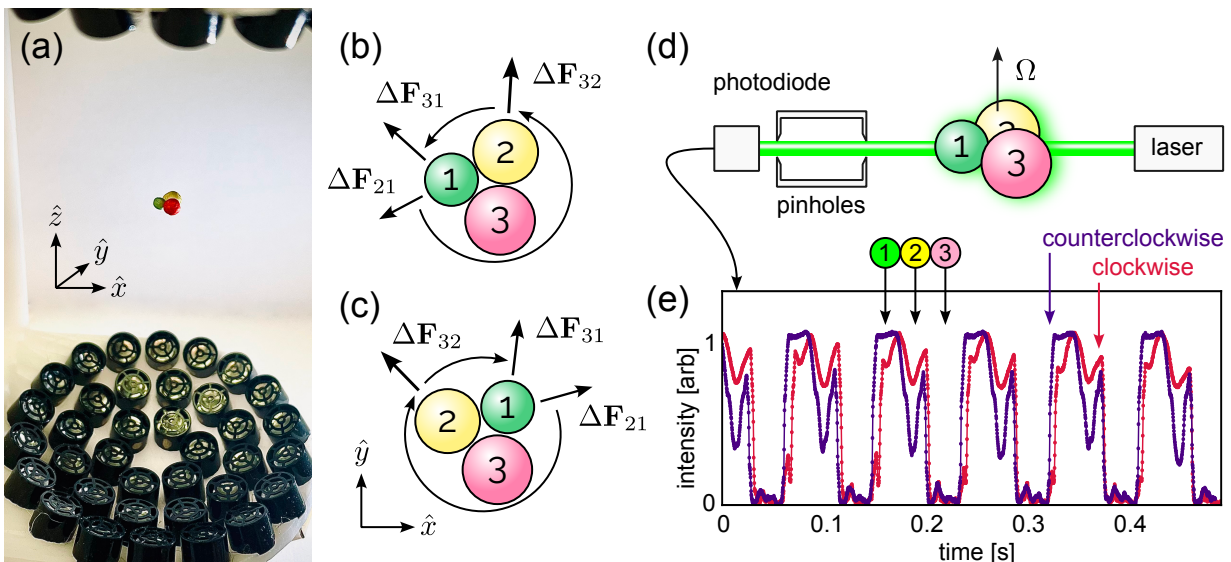


FIG. 2. Emergent activity displayed by three expanded polystyrene (EPS) beads levitated in an acoustic trap. (a) Photograph of the experimental system. Three millimeter-scale beads are trapped in a single node of a standing-wave acoustic trap at 40 kHz. (b) Schematic representation of the unbalanced forces acting on the three pairs of beads due to nonreciprocal wave-mediated interactions. The resultant torque causes the cluster to rotate about its center of mass. The cluster also would translate were it not held in place by the trap. (c) Reversing the chirality of the cluster reverses the direction of rotation. (d) Light-obscuration measurement of the cluster’s rotation. A collimated laser beam is partially blocked each time a sphere passes through the optical axis. The transmitted light is filtered by a pair of pinholes and its intensity is recorded with a photodiode. (e) Typical time traces of the recorded intensity for the two chiral configurations show the three particles moving through the beam in the sequence predicted in (b) and (c). The same rotation rate, $\Omega = (11 \pm 1)$ Hz, is recorded for both rotation directions.

which shows that the pair travels with the larger bubble in the lead. The analogous expression for dense spheres predicts the same direction of motion.

The motion induced by the exchange of scattered waves is an example of activity [2–4] in the sense that the interacting particles transduce energy from the sound wave and uses it to power their collective motion. This mechanism differs from simple driving by nonconservative acoustic forces [12, 26–28] because the structure of the wave does not dictate the direction and speed of motion; the standing wave would not move the particles at all were it not for their unbalanced influence on each other. By the same line of reasoning, this form of activity differs from the norm [2] because is not a property of the individual particles, but rather is an emergent property of the particles’ organization in the sound wave. We therefore refer to it as *emergent* activity, and note that it is likely to arise in any system where objects interact with each other by scattering waves.

Active particles often display nonreciprocal interactions [1, 29–31]. In such cases, however, the interactions’ nonreciprocity results from the particles’ activity. In the present case, conversely, the activity emerges from the nonreciprocity.

Having established that pairs of wave-coupled particles can interact nonreciprocally, we also can consider the behavior of larger clusters of particles. Wave-mediated interactions are not strictly additive because of contributions proportional to the intensity of the scattered waves.

Non-additive many-body interactions may account for the emergence of activity in large asymmetric clusters of nominally identical spheres [5, 6]. Complementary interactions arising from the scattered waves’ interference with the external wave tend to be more important for dissimilar spheres, and are pairwise additive. Superposition of these pairwise-additive contributions to the wave-mediated force should capture the principal effects of nonreciprocity and emergent activity in heterogeneous systems.

B. Experimental demonstration of emergent activity

Figure 2(a) depicts a straightforward experimental realization of nonreciprocal wave-mediated interactions and the emergent activity that they engender. The system consists of three millimeter-scale beads of expanded polystyrene [32] with a measured mass density of $\rho_j = (30.5 \pm 0.2)$ kg/m³ [33] levitated in an acoustic trap. The device is based on the standard TinyLev design [34] and consists of two banks of piezoelectric transducers (MA40S4S, Murata, Inc.) operating 40 kHz. Each bank of 36 transducers is driven sinusoidally at 10 V_{pp} by a function generator (DS345, Stanford Research Systems) and projects a traveling wave into a spherical volume of air. Interference between the counterpropagating waves creates a standing wave with an array of pressure nodes

along the instrument's vertical axis, \hat{z} .

An individual bead experiences one of the pressure nodes as a three-dimensional Hookean potential energy well [34] with a measured [33] stiffness of $50 \mu\text{N}/\text{mm}$ for a 1.5 mm-diameter bead. The well associated with one node is large enough to contain all three particles. The trio in Fig. 2 is held in contact by a combination of this primary restoring force and the secondary wave-mediated interaction. The balance of forces maintains the cluster of particles rigidly trapped in the instrument's x - y plane even when the instrument is inclined relative to gravity.

The focused acoustic trap is more complicated than the plane standing wave used to develop the theory of nonreciprocal wave-mediated forces. Nevertheless, the experimental system shares essential features with the ideal system. The particles are levitated to a common plane in a node of the pressure field. Each particle is in a position to scatter waves to both of its neighbors. Interference between the scattered waves and the incident wave gives rise to interparticle forces that act perpendicularly to the trapping force. These interparticle forces should have a nonreciprocal dependence on particle size that at least qualitatively resembles the prediction of Eq. (26)

The force diagram in Fig. 2(b) invokes the linear-superposition approximation to identify the three nonreciprocal contributions to the torque around the cluster's center. Of these, the unbalanced interaction between the largest and smallest beads, $\Delta\mathbf{F}_{13}$, is overmatched by the combined influence of the other two contributions once the beads' relative radii are taken into account. As a result, the cluster experiences a net torque in the \hat{z} direction that causes it to rotate counterclockwise, as drawn. Exchanging any two beads, as illustrated in Fig. 2(c), reverses the cluster's chirality and also is observed to reverse the direction of rotation. A typical realization of this experiment is presented in Supplementary Video 1.

We measure the cluster's rotation rate by tracking the particles [35] at 70 frames/s with a machine vision camera (Blackfly S USB 3, FLiR) outfitted with a 50 mm macro lens. To eliminate the possibility of temporal aliasing due to rapid rotation, we also record the cluster's rotation using the light obscuration system depicted in Fig. 2(d). The collimated beam from a 2 mW modular diode laser is aligned so that it is at least partially occluded when one of the particles rotates into the way. The beam has a diameter of 2 mm, which is comparable to the diameters of the beads. Beads of different sizes can be distinguished by the proportion of the beam they block. The transmitted light passes through two coaxial 250 μm -diameter pinhole apertures separated by 20 mm before being recorded by a photodiode. The photocurrent is digitized with a storage oscilloscope (TDS2002, Tektronix) at 5000 samples/s.

Typical time traces of the recorded laser intensity are plotted in Fig. 2(e) and confirm that the sense of rotation places the smallest particle in the lead, followed by the mid-sized particle and then the largest. For the specific trio of beads captured in Fig. 2(a), the typical rotation

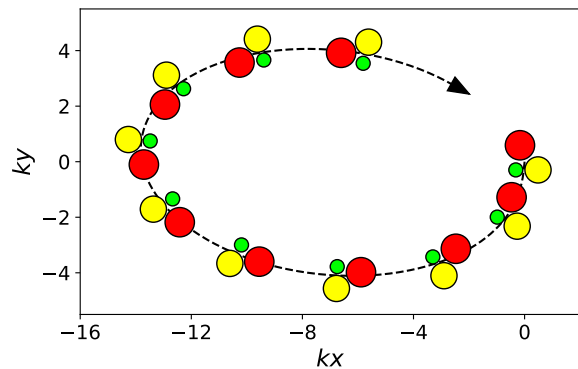


FIG. 3. Simulated dynamics of three dense spheres starting from rest in the nodal plane of a planar standing wave. The cluster is bound by conservative König interactions as it traces out an ellipse and rotates about its center of mass under the influence of nonreciprocal pair interactions and viscous drag.

rate is $\Omega = (11 \pm 1)$ Hz. The cluster rotates at the same rate in either chiral configuration, which confirms that the torque results from the particles' configuration and is not somehow encoded into the structure of the acoustic trap.

C. Simulation of emergent activity

We simulated the dynamics of a trio of dense spheres stably levitated in a plane and interacting via the nonreciprocal pair interaction described by Eq. (25). The simulation employs a velocity Verlet integrator based on the one provided by the Jax-MD molecular dynamics engine [36] augmented with Stokes drag. Each particle moves in the plane according to the equation of motion

$$m_j \ddot{\mathbf{r}}_j = -\gamma_j \dot{\mathbf{r}}_j + \sum_{i \neq j} \mathbf{F}_{ji}^K(\mathbf{r}_{ji}), \quad (29)$$

with a drag coefficient, $\gamma_j = 6\pi\eta_0 a_j$, that depends on the viscosity of air, $\eta_0 = 1.8 \times 10^{-5}$ Pas. We set the force scale to $F_0 = 10 \mu\text{N}$, which is strong enough to rigidly confine the spheres to the plane against gravity. This drive-to-drag ratio is consistent with the forces on typical experimental particles which experience a König interaction of approximately $3 \mu\text{N}$ at the nodal plane and a Stokes drag per unit velocity of $0.5 \mu\text{N} \cdot \text{s}/\text{m}$ [33]. As in the experiments, the three spheres are composed of the same material but differ in size, with reduced radii of $ka_1 = 0.3$, $ka_2 = 0.5$, and $ka_3 = 0.8$. For consistency with the experimental observations, we set the density of the particles to be 30 times that of the medium.

The typical simulation presented in Fig. 3 is performed with a time step of 140 μs . Without the confining potential of the experimental acoustic trap, the simulated trio of particles translates across the nodal plane as it rotates. The trajectory is elliptical rather than circular because the drag forces vary subtly with the configuration of the

particles relative to the direction of motion. This qualitatively resembles the translation of larger clusters of identical spheres simulated in Ref. [5] and the motion of asymmetric pairs of bubbles observed experimentally in Ref. [37]. In this case, however, the motion arises unambiguously from nonreciprocal pair interactions due to the superposition of incident and scattered waves. A typical realization of the simulation is presented in Supplementary Video 2.

V. DISCUSSION

We have established that nonreciprocity is a generic feature of the wave-mediated interactions between pairs of objects that scatter sound. Analogous nonreciprocal interactions should arise in systems supporting any sort of harmonic waves, including light [38–40] and water waves [41]. For pairs of spheres in a uniform standing wave, the wave-mediated interaction is a central force. More generally, anisotropic scattering of nonuniform waves is likely to engender wave-mediated torques on pairs of particles as well as forces.

Objects coupled by nonreciprocal forces behave in sur-

prising ways. Pairs of particles accelerate through force-free landscapes. Trios spin. Such motion is the hallmark of *emergent activity*, in which passive particles acquire the ability to transduce energy as a collective property of their state of organization.

We have demonstrated how emergent activity can arise in a harmonic wave through interference between incident and scattered fields. Similar effects also are available to systems driven by superpositions of waves with different frequencies and mode structures. Emergent activity therefore should arise naturally under quite general conditions. These observations suggest that the collective motion powered by emergent activity was available to guide natural self-organization in the epoch before biological activity evolved and so could have played a role in the emergence of life.

ACKNOWLEDGMENTS

This work was supported by the National Science Foundation under Award No. DMR-2104837. E.M.K. acknowledges support from a Simons Foundation Junior Fellowship under Grant Number 1141499.

-
- [1] A. V. Ivlev, J. Bartnick, M. Heinen, C.-R. Du, V. Nosenko, and H. Löwen, Statistical mechanics where Newton’s third law is broken, *Phys. Rev. X* **5**, 011035 (2015).
 - [2] S. Ramaswamy, The mechanics and statistics of active matter, *Annu. Rev. Condens. Matter Phys.* **1**, 323 (2010).
 - [3] M. C. Marchetti, J.-F. Joanny, S. Ramaswamy, T. B. Liverpool, J. Prost, M. Rao, and R. A. Simha, Hydrodynamics of soft active matter, *Rev. Mod. Phys.* **85**, 1143 (2013).
 - [4] C. Bechinger, R. Di Leonardo, H. Löwen, C. Reichardt, G. Volpe, and G. Volpe, Active particles in complex and crowded environments, *Rev. Mod. Phys.* **88**, 045006 (2016).
 - [5] N. St. Clair, D. Davenport, A. D. Kim, and D. Kleckner, Dynamics of acoustically bound particles, *Phys. Rev. Res.* **5**, 013051 (2023).
 - [6] M. X. Lim, B. VanSaders, A. Souslov, and H. M. Jaeger, Mechanical properties of acoustically levitated granular rafts, *Phys. Rev. X* **12**, 021017 (2022).
 - [7] S. A. Loos, S. Arabha, A. Rajabpour, A. Hassanali, and É. Roldán, Nonreciprocal forces enable cold-to-hot heat transfer between nanoparticles, *Sci. Rep.* **13**, 4517 (2023).
 - [8] M. Fruchart, C. Scheibner, and V. Vitelli, Odd viscosity and odd elasticity, *Annu. Rev. Condens. Matter Phys.* **14**, 471 (2023).
 - [9] S. Saha, J. Agudo-Canalejo, and R. Golestanian, Scalar active mixtures: The nonreciprocal Cahn-Hilliard model, *Phys. Rev. X* **10**, 041009 (2020).
 - [10] K. Yosioka and Y. Kawasima, Acoustic radiation pressure on a compressible sphere, *Acta Acust. United Ac.* **5**, 167 (1955).
 - [11] G. T. Silva, An expression for the radiation force exerted by an acoustic beam with arbitrary wavefront (L), *J. Acoust. Soc. Am.* **130**, 3541 (2011).
 - [12] M. A. Abdelaziz and D. G. Grier, Acoustokinetics: Crafting force landscapes from sound waves, *Phys. Rev. Research* **2**, 013172 (2020).
 - [13] A. A. Doinikov, Acoustic radiation pressure on a rigid sphere in a viscous fluid, *Proc. R. Soc. Lond. A* **447**, 447–466 (1994).
 - [14] O. A. Sapozhnikov and M. R. Bailey, Radiation force of an arbitrary acoustic beam on an elastic sphere in a fluid, *J. Acoust. Soc. Am.* **133**, 661 (2013).
 - [15] P. J. Westervelt, The theory of steady forces caused by sound waves, *J. Acoust. Soc. Am.* **23**, 312 (1951).
 - [16] X. Zheng and R. E. Apfel, Acoustic interaction forces between two fluid spheres in an acoustic field, *J. Acoust. Soc. Am.* **97**, 2218 (1995).
 - [17] A. A. Doinikov, Acoustic radiation interparticle forces in a compressible fluid, *J. Fluid Mech.* **444**, 1 (2001).
 - [18] P. Gabrielli and M. Mercier-Finidori, Acoustic scattering by two spheres: Multiple scattering and symmetry considerations, *J. Sound Vibrat.* **241**, 423 (2001).
 - [19] A. R. Edmonds, *Angular Momentum in Quantum Mechanics* (Princeton University Press, 1996) pp. 45–52.
 - [20] W. König, Hydrodynamisch-akustische untersuchungen, *Ann. Phys.* **279**, 43 (1891).
 - [21] V. Bjerknes, *Fields of Force* (Columbia University Press, 1906).
 - [22] A. Garcia-Sabaté, A. Castro, M. Hoyos, and R. González-Cinca, Experimental study on inter-particle acoustic forces, *J. Acoust. Soc. Am.* **135**, 1056 (2014).
 - [23] G. T. Silva and H. Bruus, Acoustic interaction forces between small particles in an ideal fluid, *Phys. Rev. E* **90**, 063007 (2014).

- [24] M. Settnes and H. Bruus, Forces acting on a small particle in an acoustical field in a viscous fluid, *Phys. Rev. E* **85**, 016327 (2012).
- [25] A. A. Doinikov, T. Micol, C. Mauger, P. Blanc-Benon, and C. Inserra, Self-propulsion of two contacting bubbles due to the radiation interaction force, *Micromachines* **14**, 1615 (2023).
- [26] L. Zhang and P. L. Marston, Angular momentum flux of nonparaxial acoustic vortex beams and torques on axisymmetric objects, *Phys. Rev. E* **84**, 065601 (2011).
- [27] T. Wang, M. Ke, W. Li, Q. Yang, C. Qiu, and Z. Liu, Particle manipulation with acoustic vortex beam induced by a brass plate with spiral shape structure, *Appl. Phys. Lett.* **109** (2016).
- [28] K. Melde, A. G. Mark, T. Qiu, and P. Fischer, Holograms for acoustics, *Nature* **537**, 518 (2016).
- [29] Z. You, A. Baskaran, and M. C. Marchetti, Nonreciprocity as a generic route to traveling states, *PNAS* **117**, 19767 (2020).
- [30] J. P. Banerjee, R. Mandal, D. S. Banerjee, S. Thutupalli, and M. Rao, Unjamming and emergent nonreciprocity in active ploughing through a compressible viscoelastic fluid, *Nat. Commun.* **13**, 4533 (2022).
- [31] A. Dinelli, J. O'Byrne, A. Curatolo, Y. Zhao, P. Sollich, and J. Tailleur, Non-reciprocity across scales in active mixtures, *Nat. Commun.* **14**, 7035 (2023).
- [32] J. Horvath, Expanded polystyrene (EPS) geofoam: an introduction to material behavior, *Geotext. Geomembr.* **13**, 263 (1994).
- [33] M. Morrell and D. G. Grier, Acoustodynamic mass determination: Accounting for inertial effects in acoustic levitation of granular materials, *Phys. Rev. E* **108**, 064903 (2023).
- [34] A. Marzo, A. Barnes, and B. W. Drinkwater, TinyLev: A multi-emitter single-axis acoustic levitator, *Rev. Sci. Instr.* **88**, 085105 (2017).
- [35] J. C. Crocker and D. G. Grier, Methods of digital video microscopy for colloidal studies, *J. Colloid Interf. Sci.* **179**, 298 (1996).
- [36] S. S. Schoenholz and E. D. Cubuk, JAX, MD: A framework for differentiable physics, *J. Stat. Mech.* **2021**, 124016 (2021).
- [37] A. A. Doinikov, Acoustic radiation forces: Classical theory and recent advances, *Recent Res. Dev. Acoust* **1**, 39 (2003).
- [38] S. Sukhov, A. Shalin, D. Haefner, and A. Dogariu, Actio et reactio in optical binding, *Opt. Express* **23**, 247 (2015).
- [39] S. Sukhov and A. Dogariu, Non-conservative optical forces, *Rep. Prog. Phys.* **80**, 112001 (2017).
- [40] X. Li, Y. Liu, Z. Lin, J. Ng, and C. T. Chan, Non-Hermitian physics for optical manipulation uncovers inherent instability of large clusters, *Nat. Commun.* **12**, 6597 (2021).
- [41] F. Jiménez-Ángeles, K. J. Harmon, T. D. Nguyen, P. Fenter, and M. O. De La Cruz, Nonreciprocal interactions induced by water in confinement, *Phys. Rev. Res.* **2**, 043244 (2020).